Geosci. Model Dev. Discuss., 6, 5423–5473, 2013
www.geosci-model-dev-discuss.net/6/5423/2013/
doi:10.5194/gmdd-6-5423-2013

Geoscientific Model Development Discussions
Open Access

Modelling methane emissions from natural wetlands: TRIPLEX-GHG model integration, sensitivity analysis, and calibration

Q. Zhu[1,3], J. Liu[2], C. Peng[3,1], H. Chen[1,3], X. Fang[4,3], H. Jiang[5], G. Yang[1], D. Zhu[3], W. Wang[3], and X. Zhou[3]

[1]State Key Laboratory of Soil Erosion and Dryland Farming on the Loess Plateau, Northwest A&F University, Yangling, Shaanxi 712100, China
[2]Contractor, Western Geographic Science Center, US Geological Survey, Menlo Park, CA 94025, USA
[3]Department of Biology Science, Institute of Environment Sciences, University of Quebec at Montreal, Montreal H3C 3P8, Canada
[4]College of Earth Science and Engineering, Hohai University, Nanjing, 210098, China
[5]International Institute for Earth System Science, Nanjing University, Hankou Road 22, Nanjing 210093, China

Received: 31 August 2013 – Accepted: 18 September 2013 – Published: 4 November 2013
Correspondence to: C. Peng (peng.changhui@uqam.ca) and Q. Zhu (qiuan.zhu@gmail.com)
Published by Copernicus Publications on behalf of the European Geosciences Union.

GMDD
6, 5423–5473, 2013

Abstract

This paper introduces TRIPLEX-GHG, a new process-based model framework used to quantify terrestrial ecosystem greenhouse gas dynamics by incorporating both ecological drivers and biogeochemical processes. TRIPLEX-GHG was developed from the Integrated Biosphere Simulator (IBIS), a dynamic global vegetation model, coupled with a new methane (CH_4) biogeochemistry module (incorporating CH_4 production, oxidation, and transportation processes) and a water table module to investigate CH_4 emission processes that occur in natural wetlands. Sensitivity analysis indicates that the most sensitive parameters to use to evaluate CH_4 emission processes from wetlands are *r* (defined as the CH_4 to CO_2 release ratio) and Q10 in CH_4 production process. These two parameters were subsequently calibrated to data obtained from 19 sites collected from approximately 35 studies across different wetlands globally. Having a heterogeneous spatial distribution, *r* and Q10 parameters ranged from 0.1 to 0.55 with a mean value of 0.25 and from 1.6 to 4.5 with a mean value of 2.48, respectively. The model performed well when simulating magnitude and capturing temporal patterns in CH_4 emissions from natural wetlands despite failing to capture CH_4 emission pulses in certain cases. Results suggest the model can be applied to different wetlands under varying conditions and is also applicable for global scale simulations.

1 Introduction

An important greenhouse gas, methane (CH_4) undergoes radiative forcing on a molecular level at an approximate order of magnitude twenty times that of carbon dioxide (CO_2) (Van Ham et al., 2000; Denman et al., 2007). Atmospheric CH_4 originates from biogenic sources that account for greater than 70 % of total global CH_4 emissions and the natural wetlands are the largest individual CH_4 source (Denman et al., 2007). Wetlands also play a vital role in global carbon (C) cycling, being an important terrestrial ecosystem component in addition to the role it plays in the CH_4 budget (Zhang et al., 2002; Denman et al., 2007). Wetlands contribute largely to interannual variations and

GMDD
6, 5423–5473, 2013

anomalies of atmospheric CH_4 concentrations (Walter et al., 2001a). Owing to this, it is vital to improve existing CH_4 emission quantification methods for wetlands to better understand the global CH_4 budget (Chen et al., 2013).

Over the decades, three approaches have generally been used in estimating CH_4 wetland emissions, including: (1) extrapolation from direct flux measurements and observations, (2) process-based modelling (bottom-up approach), and (3) inverse modelling and satellite observations (top-down approach) (Arneth et al., 2010; Denman et al., 2007). The first approach can be unreliable in scaling from point measurements up to regional or global scales due to limitations in spatial and temporal coverage of measurements (Cao et al., 1996). The currently used top-down approach – generally believed proficient in covering large regions – may inadvertently include some incomplete observations and error amplifications during inverse modelling processes (Chen and Prinn, 2005; Denman et al., 2007). Process-based models can be used to improve CH_4 emission estimation under different climatic regimes and at the same time cope with the complex interactions that take place between soil, vegetation, and hydrology under CH_4 production and consumption processes. The development and application of process-based models could be a practical alternative approach when extrapolating site scale to regional or global scale results (Cao et al., 1996; Li, 2000; Zhang et al., 2002).

Several process-based models have previously been developed to estimate global CH_4 emissions. Each has its own strategy and features to deal with wetland system complexity and CH_4 flux processes (Li, 2000; Meng et al., 2012; Walter and Heimann, 2000; Zhuang et al., 2004). Cao et al. (1995) developed a CH_4 emissions model for rice paddies based on C substrate level, soil organic matter (SOM) degradation, and environmental control factors. They have since improved their model and applied it to natural wetlands, coupling datasets of climate, vegetation, soil, and wetland distribution to use in global CH_4 emission simulations (Cao et al., 1996). Walter and Heimann (2000) developed a one-dimensional process-based climate-sensitive model that explicitly describes three different transport mechanisms by which to estimate natural

GMDD
6, 5423–5473, 2013

wetland CH_4 emissions. This model – using a simple hydrologic module to simulate water tables – was applied at a global scale to estimate long-term CH_4 emissions from natural wetlands (Walter et al., 2001a, b). Li (2000) developed a denitrification-decomposition model (DNDC) to simulate trace gas emissions (including CH_4) from agricultural ecosystems. Zhang et al. (2002) adopted the DNDC model and some of its key components to simulate wetland ecosystem emissions. Zhuang et al. (2004) integrated CH_4 emission and consumption modules into the Terrestrial Ecosystem Model (TEM) to estimate net CH_4 emissions in Northern Hemisphere high-latitude soils throughout the twentieth century. Moreover, van Huissteden et al. (2006) developed a process model (PEATLAND) to simulate CH_4 flux from peat soils under different water table management scenarios. This model has since been up-scaled by Petrescu et al. (2010). to use for global boreal and arctic wetlands. After integrating permafrost dynamics, peatland hydrology, and peatland vegetation into the dynamic global vegetation model Lund-Potsdam-Jena (LPJ) (Wania et al., 2009b), Wania et al. (2010) integrated a CH_4 emissions module into the enhanced LPJ model to simulate CH_4 emissions from northern peatlands. This model had then been modified to simulate global net CH_4 emissions for various ecosystems (Spahni et al., 2011). To explain spatial and temporal variation in CH_4 emissions and characterize uncertainties and feedbacks between CH_4 flux and climate, Riley et al. (2011) developed a CH_4 biogeochemistry model (CLM4Me) and integrated it into the land component of the Community Earth System Model (CESM). Meng et al. (2012) later made certain modifications and further analyses based on this model.

Although many process-based CH_4 wetland models have been developed, considerable uncertainties remain in CH_4 emissions modelling on a global scale (Petrescu et al., 2010). The Wetland and Wetland CH_4 Inter-comparison of Models Project (WETCHIMP), which simulates and compares large-scale wetland characteristics and corresponding CH_4 emissions, reported that large uncertainties indeed still exist when estimating CH_4 emissions (Wania et al., 2013; Melton et al., 2013). These uncertainties are generally introduced from large temporal and spatial

GMDD
6, 5423–5473, 2013

variations in CH_4 flux – the complex processes that underlie CH_4 emissions – and also the limited inherent range of field and laboratory measurements (Arneth et al., 2010; Spahni et al., 2011; Wania et al., 2010; Denman et al., 2007; Meng et al., 2012). Since no simple relationship exists between environmental factors and CH_4 emission processes for wetlands, the development of process-based CH_4 emission models is critical (Ito and Inatomi, 2012; Walter and Heimann, 2000). Coupling the CH_4 emissions module into the Dynamic Global Vegetation Model (DGVM) would be an efficient approach to reflect interactions between hydrology, vegetation, soil, and CH_4-related processes, subsequently reducing uncertainties in CH_4 emission estimation at different spatial and temporal scales (Arneth et al., 2010; Wania et al., 2010; Tian et al., 2010). It would also be a practical approach to apply when predicting spatial and temporal patterns of CH_4 emissions under different future climate change scenarios (Gedney et al., 2004; Shindell et al., 2004; Tian et al., 2010). DGVM generally combines vegetation dynamics, biogeochemistry, and biogeography processes to project terrestrial ecosystem response under conditions of rapid climate change (Cramer et al., 2001; Prentice et al., 1989). Wania et al. (2010) integrated a CH_4 emissions model directly into a DGVM for the first time. The current study introduces a new model development framework of TRIPLEX-GHG in which CH_4 emissions model based on a synthesis of the previous studies discussed and the model was integrated into a DGVM called the Integrated Biosphere Simulator (IBIS). IBIS is designed to integrate a variety of terrestrial ecosystem phenomena within a physically consistent modelling framework. It represents land surface processes, canopy physiology, vegetation phenology, long-term vegetation dynamics, and C cycling (Foley et al., 1996; Kucharik et al., 2000). In addition, a water table simulation module based on an approach developed by Granberg et al. (1999) was integrated into the hydrological component of IBIS in this study. For this study, a CH_4 emissions model was constructed for natural wetlands and integrated into IBIS. Model parameter sensitivity was analyzed, and the model was tested on different wetland sites throughout the globe.

GMDD
6, 5423–5473, 2013

2 Model description and key processes

The TRIPLEX-GHG model framework (Peng et al., 2013) – a new development in the TRIPLEX model family (Peng et al., 2002) – is based on the legacy of well-established and published models that include IBIS (Foley et al., 1996), DNDC (Li, 2000), TRIPLEX (Peng et al., 2002), and CASACNP (Wang et al., 2010). TRIPLEX-GHG shares many key features with IBIS. However, the scope of this study was only to introduce the development of the new wetland water table module and the methanogenesis module of TRIPLEX-GHG integrated into IBIS. The basic concept and structure of CH_4 emission and water table module and their integration into IBIS are presented in Fig. 1.

2.1 Water table module

IBIS, being a DGVM, represents vegetation with plant functional types (PFT) characterized in terms of biomass and LAI to simulate changes in vegetation structure on an annual time step through PFT sunlight and water competition (Foley et al., 1996; Kucharik et al., 2006, 2000). For wetland simulations, a new PFT was added in this model that only applies to wetlands. Most of these PFT phenological and physiological parameters were adopted from the C3 grass PFT in the original IBIS model. The assumption made by Wania et al. (2009a) was followed: to incorporate inundation stress effects on gross primary production (GPP) of the added PFT. Wania et al. (2009a) summarized that sphagnum and C3 graminoids photosynthesis will increase during times when water content or the water table rises or decrease during times when water content or the water table drops.

Since the water table is an essential factor in determining anoxic and oxic soil zone extent – where CH_4 is produced and oxidized, respectively – a water table simulation module was integrated into IBIS. The module primarily follows the approach developed by Granberg et al. (1999). This approach has been applied in studies of Zhuang et al. (2004), Weiss et al. (2006), and Wania et al. (2009b). Although applications of

GMDD
6, 5423–5473, 2013

the water table simulation approach by Granberg et al. (1999) have been primarily carried out in peatland or mires, the method was extended for water table simulations of natural wetlands for this study. Water balance is the basis of water table simulations. Instead of the six soil layers used in the original IBIS model, two layers were specified for wetlands: the anoxic zone (saturated zone) and the oxic zone (unsaturated zone), separated by water table surface. Positioning of water table changes is subject to soil moisture change, i.e., the input and output volume of water in a specific location. The assumption is that standing water can occur above the land surface and that the drainage process through the bottom of the soil layers can be omitted. When water table position is higher than maximum standing water, excess water will be yielded as runoff. The water budget in the wetland soil profile was derived from the deficit of water input (precipitation) and water output (evapotranspiration and runoff). The water table is estimated by the equation provided below, which was also described in studies by Granberg et al. (1999) and Wania et al. (2009b):

$$\text{Water\_Table} = \begin{cases} V_{\text{tot}} - Z_{\text{acro}}\phi & \text{if} \quad \text{WT} > 0 \\ -\sqrt{\frac{3.0\cdot(Z_{\text{acro}}\phi - V_{\text{tot}})}{2.0\cdot A_z}} & \text{if} \quad \text{WT} \le Z_{\theta\text{s,min}} \\ -\frac{3.0\cdot(Z_{\text{acro}}\phi - V_{\text{tot}})}{2.0\cdot(\phi - \theta_{\text{s,min}})} & \text{if} \quad \text{WT} > Z_{\theta\text{s,min}} \end{cases} \quad (1)$$

where V_{tot} is total water content in the soil profile, Z_{acro} is the maximum water table depth (30 cm, adopted from Granberg et al., 1999), ϕ is the soil porosity, $\theta_{\text{s, min}}$ is the minimum volumetric water content at the soil surface (0.25, adopted from Granberg et al., 1999), $Z_{\theta\text{s,min}}$ is the maximum depth where evaporation influences soil moisture (10 cm, adopted from Granberg et al., 1999). A_z is the gradient in the linearly decreasing interval, calculated as: $A_z = (\phi - \theta_{\text{s, min}})/Z_{\theta\text{s,min}}$. A negative or a positive value of the water table indicates that the water table is below or above the soil surface, respectively.

GMDD
6, 5423–5473, 2013

2.2 Methane module

The CH_4 emissions module was adapted and integrated from a number of studies and models (Li, 2000; Riley et al., 2011; Spahni et al., 2011; Walter and Heimann, 2000; Wania et al., 2010; Zhang et al., 2002). Three major processes that include CH_4 production, CH_4 transport (ebullition, diffusion, and plant mediated transport), and CH_4 oxidation were coupled with IBIS. CH_4 is produced in each soil layer when soil conditions are favourable. Change in CH_4 for each time step in each soil layer is determined by CH_4 production magnitude (Pro_{CH_4}), oxidation (Oxi_{CH_4}), and three way transportation (Ebu_{CH_4}, Dif_{CH_4}, and PMT_{CH_4}). For each soil layer, change in CH_4 content is the difference between production (Pro_{CH_4}) and consumption/emission (sum of Oxi_{CH_4}, Ebu_{CH_4}, Dif_{CH_4}, and PMT_{CH_4}). Total CH_4 flux to the atmosphere is the sum of Ebu_{CH_4}, Dif_{CH_4}, and PMT_{CH_4}.

2.2.1 Methane production

CH_4 production is considered as the final stage of organic matter mineralization in anaerobic ecosystems, such as wetlands (Cao et al., 1996). It is usually considered as related to the relationship between plant primary production, decomposable soil organic carbon, CO_2 exchange rates, or soil heterotrophic respiration rates (Walter and Heimann, 2000; Walter et al., 2001a; Whiting and Chanton, 1993; Cao et al., 1996; Sass et al., 1990). CH_4 production depends not only on carbon substrate supply from plant primary production, but also on soil environmental conditions, such as the water table, soil temperature, and hydrological regimes (Cao et al., 1996; Moore and Knowles, 1990; Walter and Heimann, 2000).

Since CH_4 is considered as the end production in the biological reduction of CO_2 or organic carbon under anaerobic conditions (Li, 2000; Nouchi et al., 1994), it was assumed here that CH_4 production is directly related to heterotrophic respiration and there are therefore no delays between fermentation and CH_4 production (Riley et al., 2011). CH_4 production was calculated as a proportion of heterotrophic respiration

GMDD
6, 5423–5473, 2013

(CO_2-C) along with soil temperature, Eh, and pH modification factors.

$$\mathrm{Pro}_{CH_4} = R_H \cdot r \cdot f_{ST} \cdot f_{pH} \cdot f_{Eh} \quad (2)$$

where R_H is the soil heterotrophic respiration rate, calculated as the change in soil carbon pool size for each time step by the biogeochemical module in IBIS. f_{ST}, f_{pH}, and f_{Eh} represent CH_4 production factors of soil temperature, pH, and redox potential, respectively. r is the release ratio of CH_4 to CO_2.

Studies have shown that CH_4 production below zero is small or significantly lower than that found during growing seasons (Shannon and White, 1994; Whalen and Reeburgh, 1992). Moreover, studies also suggest that CH_4 emissions during winter are actually produced during the previous summer and stored in the soil profile (Dise, 1992; Melloh and Crill, 1996). Therefore, CH_4 production was only permitted in the module when soil temperature was above the freezing point and below an extremely high temperature limit. The relationship between soil temperature and CH_4 production was adapted from Zhang et al. (2002) as described below:

$$f_{ST} = \begin{cases} 0 & \text{if } T_{soil} < 0 \\ 0 & \text{if } T_{soil} > T_{max} \\ \mathrm{vt}^{\mathrm{xt}} \cdot \exp(xt \cdot (1 - vt)) & \text{if } 0 \le T_{soil} \le T_{max} \end{cases} \quad (3)$$

where

$$\mathrm{vt} = \left(\frac{T_{max} - T_{soil}}{T_{max} - T_{opt}} \right) \quad (4)$$

$$\mathrm{xt} = (\log(Q_{10}) \cdot (T_{max} - T_{opt}))^2 \left(1.0 + \left(1.0 + 40.0/(\log(Q_{10}) \cdot (T_{max} - T_{opt}))\right)^{1/2}\right)^2 / 400.0 \quad (5)$$

and T_{max} and T_{opt} are the highest temperature and optimum temperature for CH_4 production with values of 45 °C and 25 °C, respectively. T_{soil} is soil temperature.

GMDD
6, 5423–5473, 2013

Temperature effects, usually represented by Q10, have high degrees of uncertainty with a broad ranges (Westermann, 1993; Dunfield et al., 1993). Cao et al. (1996) used a Q10 value of 2.0 while Walter and Heimann (2000) and Walter et al. (2001a) used a Q10 value of 6.0. Methanogenesis has a Q10 value range between 1.2 and 3.5 in laboratory studies (Cao et al., 1996). Some studies have shown the range of observed Q10 values ranging from 1.7 to 16 (Dunfield et al., 1993; Valentine et al., 1994). Zhuang et al. (2004) used an ecosystem-specific Q10 coefficient to evaluate soil temperature effects on CH_4 production at northern high latitudes. For this study, a base Q10 value of 3.0 was used (Zhang et al., 2002) for simulations at different calibration sites. Obtaining an optimal value at each individual site during parameter calibration was then attempted.

Soil pH affected methanogenesis with a tolerance range between 5.5 and 9.0 while optimal values ranged between 6.4 and 7.8 with peak values ranging between 6.9 and 7.1 (Cao et al., 1995; Wang et al., 1993). Walter and Heimann (2000) included the effects of pH on CH_4 production in the tuning parameter. The approach by Cao et al. (1995) was adopted here to express the relationship between soil pH and CH_4 production:

$$f_{pH} = \begin{cases} 0 & \text{if } pH_{soil} > pH_{high} \text{ or } pH_{soil} < pH_{low} \\ \left(\frac{pH_{soil}-pH_{low}}{pH_{opt}-pH_{low}}\right) \cdot \left(\frac{pH_{high}-pH_{soil}}{pH_{high}-pH_{opt}}\right)^{\frac{pH_{high}-pH_{opt}}{pH_{opt}-pH_{low}}} & \end{cases} \quad (6)$$

where pH_{low} and pH_{high} represent low (4.0) and high (9.0) limitations of pH effect intervals. The optimal value was set at 7.0.

Inundation will cause low redox potential and promote an anaerobic soil environment that will stimulate methanogenesis. Cao et al. (1995) assumed CH_4 production processes would be switched on or off with redox potential below or above −200 mV, respectively. A linear relationship between soil water table position and CH_4 production was used to represent the effects of redox potential in another study (Cao et al., 1996). Li (2000) assumed that CH_4 production takes place as soon as the soil Eh

GMDD
6, 5423–5473, 2013

level is 150 mV or lower. Used here was the relationship between redox potential and CH_4 production generalized by Zhang et al. (2002), based on studies by Fiedler and Sommer (2000) and Segers (1998). When redox potential is within a range between −200 mV and −100 mV, its effect on methanogenesis diminishes linearly from 1 to 0. Otherwise, the factor is equal to 1.0 and 0.0 when redox potential is less than −200 mV and greater than −100 mV, respectively. Eh relates to days of continued inundation. The soil layer is considered inundated when water-filled pore space (WFPS) is greater than 0.95. The Eh calculation is also based on the root distribution and position of the water table (Zhang et al., 2002; Zhuang et al., 2004; Segers and Kengen, 1998).

Cao et al. (1995, 1996) used a constant ratio to represent the proportion of decomposed organic carbon that can be converted to CH_4. Walter et al. (Walter and Heimann, 2000; Walter et al., 2001a) used a tuning parameter to adjust the amplitude of simulated CH_4 emissions. The parameter was calculated using a simple multiple linear regression of soil organic carbon and mean annual temperature. Zhuang et al. (2004) used an ecosystem-specific potential rate for CH_4 production. Adopted here was the assumption used in the CLM4Me (Riley et al., 2011; Meng et al., 2012) and LPJ-WHyMe (Spahni et al., 2011; Wania et al., 2010) models where CH_4 production within the anaerobic portion of the soil column relates to soil heterotrophic respiration, and that the soil substrate for methanogenesis is considered as a fraction of soil heterotrophic respiration. The release ratio of CH_4 to CO_2 in the CH_4 production equation is an adjustable parameter and determined by parameter fitting as described by Wania et al. (2010).

2.2.2 Methane oxidation

CH_4 is oxidized by aerobic methanotroph activity in the soil, taking place in the unsaturated zone above the water table (Zhuang et al., 2004; Cao et al., 1996; Li, 2000). Cao et al. (1996) calculated the rate of CH_4 oxidation based on a linear relationship with GPP. Li (2000) calculated the CH_4 oxidation rate as a function of soil CH_4 concentration and Eh. Given that CH_4 oxidation is primarily controlled by CH_4

GMDD
6, 5423–5473, 2013

concentration, redox potential, and soil temperature (Segers, 1998), the equation used here is as follows:

$$\mathrm{Oxi}_{\mathrm{CH_4}} = C_{\mathrm{CH_4}} \cdot f_{\mathrm{CH_4}} \cdot f_{\mathrm{ST}} \cdot f_{\mathrm{Eh}} \quad (7)$$

The CH_4 concentration factor (f_{CH_4}) is represented by a Michaelis–Menten kinetic relationship: $C_{CH_4}/(K_{CH_4} + C_{CH_4})$ where C_{CH_4} is the CH_4 concentration and K_{CH_4} is the half-saturation coefficient with respect to CH_4 concentration (Riley et al., 2011; Walter and Heimann, 2000). A Q10 value of 2.0 based on results from previous studies (Segers, 1998; Walter and Heimann, 2000; Zhang et al., 2002) was used to quantity soil temperature effects on CH_4 oxidation (f_{ST}). Redox potential effects on CH_4 oxidation (f_{Eh}) was adopted from a general relationship between redox potential and CH_4 oxidation reported by Zhang et al. (2002), which was taken from Fiedler and Sommer (2000) and Segers (1998). The f_{Eh} was set to zero and 1.0 when Eh was below −200 mV and above 200 mV, respectively. It was represented in the range of −200 mV to −100 mV and −100 mV to 200 mV by two simple linear functions, which were varied from 0 to 0.75 and from 0.75 to 1, respectively.

2.2.3 Methane emission processes

In earlier studies, no specific CH_4 emission process in CH_4 modelling existed (Cao et al., 1995, 1996). Gradually, major CH_4 emission processes, including diffusion, ebullition, and plant mediated transportation, were formulated by the release of more recent models (Li, 2000; Riley et al., 2011; Walter and Heimann, 2000; Wania et al., 2010). For examples, Li (2000) used a highly simplified scheme to model CH_4 diffusion between soil layers, assuming that ebullition occurs at the surface layer and that plant mediated transportation is a function of CH_4 concentration and plant aerenchyma; Walter & Heimann (2000) calculated methane diffusion using a function based on Fick's first law where CH_4 ebullition occurs when CH_4 concentration in a specific soil layer exceeds a certain threshold and where CH_4 plant mediated transport is

GMDD
6, 5423–5473, 2013

quantified by factors related to plant density, plant type, root distribution, plant growth, and rhizospheric oxidation.

CH_4 diffusion between soil layers was estimated here using Fick's law based on the CH_4 concentration gradient in the soil profile (Walter and Heimann, 2000; Zhuang et al., 2004). The diffusion coefficient for each soil layer was modelled as follows:

$$D_i = D_a \cdot f_{coarse} \cdot f_{tort} \cdot \text{SoilPoro} \cdot (1 - \text{WFPS}_i) + D_w \cdot \text{WFPS}_i \quad (8)$$

where D_a and D_w are the CH_4 molecular diffusion coefficients in the air with a value of $0.2\,cm^2\,s^{-1}$ and in water with a value of $0.00002\,cm^2\,s^{-1}$, respectively (Walter and Heimann, 2000). D_a and D_w reflect differences in the rate of CH_4 molecular diffusion through unsaturated vs. saturated soil layers. f_{coarse} is the relative volume of coarse pores depending on soil texture (Zhuang et al., 2004). f_{tort} is the tortuousity coefficient with a value of 0.66 (Walter and Heimann, 2000). Lastly, WFPS is the water filled pore space.

Being a relatively rapid channel for CH_4 emissions, bubbles will form as soon as CH_4 concentrations in the soil profile exceeds a certain threshold (Walter and Heimann, 2000). Walter and Heimann (2000) used the vegetation cover fraction to estimate the CH_4 threshold. For CH_4 ebullition emission processes, a constant threshold value of 750 umol L^{-1} was used in the current study.

Vascular plants provide an effective pathway for CH_4 transport to the atmosphere (Shannon et al., 1996; Walter and Heimann, 2000). Adopted here was the assumption by Walter and Heimann (2000) that plant-mediated flux is proportional to CH_4 concentration in the soil and is related to the concentration gradient between the soil and the atmosphere. A simple equation was used to describe plant-mediated emissions based on the plant aerenchyma factor:

$$\text{PMT}_{CH_4} = f_{rhi} \cdot f_{aer} \cdot \text{CH}_{4gra} \quad (9)$$

where f_{rhi} is the rhizospheric oxidation factor, suggesting that a relatively large proportion of CH_4 will be oxidised in the highly oxic rhizospheric zone before entering

GMDD
6, 5423–5473, 2013

plant tissue (Wania et al., 2010). The rhizospheric oxidation fraction is dependent on plant type and can range between 20 % and 100 % (Wania et al., 2010; Strom et al., 2005). For this factor, a constant value of 0.5 was used here (Zhang et al., 2002). f_{aer} is the plant aerenchyma factor estimated as a function of root length density (Zhang et al., 2002). CH_{4gra} is the CH_4 concentration deficit factor between the soil profile and the atmosphere.

3 Data

3.1 Input data

Data related to climate, CO_2 concentration, soil property, and topography are described below.

The CRU-TS 3.1 Climate Database (http://badc.nerc.ac.uk/data/cru) was adopted to construct monthly climate input data for the simulation. The original CRU-TS 3.1 Database covered a monthly time series from 1901 to 2009 with a global spatial resolution of 0.5°. Variables selected include cloud cover, diurnal temperature range, precipitation, temperature, vapour pressure, and wet-day frequency. Used for the model spin-up period was 30 yr (1961–1990) means of the CRU data (http://www.ipcc-data.org/obs/get_30yr_means.html), including cloud cover, diurnal temperature range, precipitation, temperature, vapour pressure, wet-day frequency, and wind speed.

CO_2 concentration data for the simulation period were composed of two parts. Observed CO_2 concentrations were used for the period covering 1958–2009, derived by Keeling et al. (2005) from in situ air measurements taken at Mauna Loa Observatory, Hawaii. CO_2 concentrations before 1958 were adopted from the IS92a global [CO_2] yearly dataset, derived using a spline fit of Mauna Loa and ice core data (Enting et al., 1994).

The soil classification map used was based on the Digital Soil Map of the World (DSMW), generated from the FAO-UNESCO Soil Map of the World (http://www.fao.org/

GMDD
6, 5423–5473, 2013

geonetwork/srv/en/metadata.show?id=14116). DSMW attributes were connected with the soil properties dataset contributed by Batjes (2006) that describes characteristics of soil texture (soil clay, sand, and silt fraction) and soil pH. A global soil dataset (IGBP-DIS, 2000) was adopted to generate soil carbon data for model initialization.

A global digital elevation model (DEM) with an approximate 1 km spatial resolution (GTOPO30) was used for the topographic input data.

3.2 Site data for model sensitivity analysis, parameter fitting, and calibration

Observed CH_4 emissions data of natural wetlands based on previous studies or field work (19 sites worldwide across an approximate 35 studies) were collected for model sensitivity analysis, parameter fitting, and calibration. Information related to these wetland sites, including location, wetland type, measurement method, and references are summarised in Table 1. Sites have a wider geographical spread over low- to mid- to high-latitude regions (Fig. 2).

3.3 Sensitivity index for initial sensitivity analysis

Sensitivity is generally expressed as the ratio between a relative change of model output and a relative change of a parameter. The sensitivity index described in Lenhart et al. (2002) was used to quantify sensitivity in this study. The sensitivity index (I) is expressed as a finite difference in approximation of a partial derivative, which indicates the dependence of a variable (y) from a parameter (x).

$$I = \frac{(y_2 - y_1)/y_0}{2\Delta x/x_0} \tag{10}$$

where y_0 is the model output with an initial parameter of x_0. The initial parameter value varied by $\pm\Delta x$ ($x_1 = x_0 - \Delta x$ and $x_2 = x_0 + \Delta x$) between the corresponding yielding values y_1 and y_2. The sensitivity index symbol (I) indicates the direction of model reaction to parameter change. According Lenhart et al. (2002), calculated sensitivity

GMDD
6, 5423–5473, 2013

indices are ranked into four classes. Model sensitivity for a specific parameter is low to negligible when the absolute value of the sensitivity index is less than 0.05 but very high when the absolute value of the sensitivity index is greater than or equal to 1.0.

4 Results

4.1 Model sensitivity analysis and parameter fitting

4.1.1 Initial sensitivity analysis

Table 2 lists the major parameters in the CH_4 module described in Sect. 2.2. Some of the parameters adopted values that have been fully discussed and supported in previous studies. Based on analyses carried out in previous studies, only three parameters (the release ratio of CH_4 to CO_2, Q10 for CH_4 production, and Q10 for CH_4 oxidation) were selected for sensitivity experiments in order to make sensitivity analysis processes simple and efficient.

Changing scenarios for values of selected parameters for the sensitivity test are listed in Table 3. The base value (e.g., initial value) and range for each parameter were adopted from previous studies. Two sites were selected (Stordalen and BOREAS SSA, Table 1) for sensitivity analysis testing.

For the model, sensitivity analysis results indicate the release ratio of CH_4 to CO_2 (Fig. 3a1 and a2) and Q10 for CH_4 production (Fig. 3c1, d1, c2 and d2) were very sensitive. However, the sensitivity index of Q10 for CH_4 oxidation was less than 0.05 during most months for the two test sites (Fig. 3b1 and b2). This implies a very low model sensitivity of the Q10 parameter for the CH_4 oxidation process. Seasonal patterns of sensitivity indices show that the model was more sensitive to parameters during winter in most situations. The sensitivity level for the Q10 in methane production process was increasing with the changing magnitude of the Q10 value (Fig. 3d1 and d2). Although the sensitivity index of Q10 for CH_4 oxidation was higher than 1.0 during

GMDD
6, 5423–5473, 2013

a handful of months at site BOREAS SSA, it was much lower compared to the other two parameters. To simplify parameter fitting and make processes efficient as well as to assess model performance while reducing fluctuating parameters to as few as possible, Q10 for CH_4 oxidation was set as a constant value (2.0) and only two adjustable parameters were chosen (the release ratio of CH_4 to CO_2 and Q10 for CH_4 production) during parameter fitting and model calibration discussed below.

4.1.2 Model parameterization and calibration

Direct measured forcing data (e.g., climate data, soil data, etc.) was unavailable for the 19 test sites (Table 1). Therefore, each site was located on global input data layers (described in Sect. 3) and used the corresponding data for the simulation of each individual site. Observation period modelling results were used for parameter fitting and model performance evaluation. Monthly and yearly emission rates were calculated from simulated daily rates when comparing monthly and yearly observed data.

Many of the sites listed in Table 1 were also used in other CH_4 emission modelling tests. Detailed information could be found in given citations. Since there were no observed detailed individual plot data in the studies carried out in the Amazon Basin (Bartlett et al., 1990, 1988; Devol et al., 1988; Melack et al., 2004) and South Florida (Burke et al., 1988; Harriss et al., 1988), with only emission rate throughout the regions, emission rates were compared on a regional scale between prediction and estimation, based on field work (Fig. 2). For some sites where different studies were carried out by different groups in the same or different time period (e.g., Sanjiang plain, Stordalen, Minnesota, etc., Table 1), comparisons were made between the same modelled results and those results from different studies.

Calibration sites were categorized into five geographical regions: China, Europe, United States of America, Canada, and the Southern Hemisphere (Table 1). Parameters r (the release ratio of CH_4 to CO_2) and Q10 for CH_4 production were adjusted to yield the best agreement for each site between simulation and observations (Figs. 4–8). The final value for each site is listed in Table 4. The release ratio of CH_4

GMDD
6, 5423–5473, 2013

to CO_2 ranged from 0.1 to 0.55 with a mean value of 0.25, and the Q10 value for CH_4 production ranged from 1.6 to 4.5 with a mean value of 2.48.

4.2 Model performance across selected regions

4.2.1 China

Two sites were selected to test the model, one in northeast China and one in the Qinghai-Tibet Plateau. This was because natural wetlands and floodplains in China are primarily located in these two regions. Figure 4a and b show comparisons between field measurements and model simulations in the Sanjiang Plain in northeast China. Figure 4a shows mean CH_4 emissions from wetlands of different plant types in a study by Huang et al. (2010) compared to CH_4 emission rates of inundated marshes in a study by Song et al. (2009). CH_4 emission rates reported by Huang et al. (2010) were relatively low. Simulated CH_4 emissions for 2002–2003 were much higher than observed. For 2003–2004, CH_4 emission rates were higher for Song et al. (2009) by an approximate magnitude of 2.5 compared to Huang et al. (2010). Simulated results were within range of these two independent studies.

Observed data (provided in Fig. 4b) were digitized from each study. The wetland plant type used in the studies was *Carex lasiocarpa* (Ding et al., 2004; Yang et al., 2006; Cui, 1997; Hao et al., 2004; Wang et al., 2002b). The peak value (growing season) of observed data in a study by Ding et al. (2004) was slightly higher than modelled results for 2001–2002 while observed data in a study by Hao et al. (2004) was lower than those reported in a study by Ding et al. (2004) as well as this study's simulation for 2002. Modelled monthly CH_4 emission rates stood in good agreement with studies by Cui (1997) and Yang et al. (2006) for 1995 and 2003, respectively.

For those studies carried out in the Qinghai-Tibet Plateau, modelled peak values were slightly higher than observed data collected from studies with the exception of a 2005 comparison reported in a study by Chen et al. (2008). It was observed that reported CH_4 emission rates by Chen et al. (2008) for 2005 were much higher than their

GMDD
6, 5423–5473, 2013

reported 2006 emission rates and also higher than emission rates observed by Wang et al. (2002a) and Ding et al. (2004) even though site locations (provided in Fig. 4c, d) were situated very close to each other. Figure 4 also shows that natural wetland CH_4 emission rates in northeast China were higher by several orders of magnitude compared to the Qinghai-Tibet Plateau.

4.2.2 Europe

Data on five natural European wetland sites were collected, including one subarctic mire site and one boreal mire site in Sweden (Jackowicz-Korczyński et al., 2010; Svensson et al., 1999; Granberg et al., 2001), one pine fen and one boreal fen site in Finland (Rinne et al., 2007; Saarnio et al., 1997), and one ombrotrophic bog site in Russia (Panikov and Dedysh, 2000). Observed data were obtained or digitized from the above-mentioned citations (listed in Fig. 5). Svensson et al. (1999) and Jackowicz-Korczyński et al. (2010) made CH_4 emission measurements at the same site during different time periods (Fig. 5a, b). The mean emission rate of four wet and semi-dried sites in Svensson et al.'s (1999) study and data observed with automatic chamber system in Jackowicz-Korczyński et al.'s (2010) study were used for comparison (Fig. 5a, b). CH_4 emission rates ranged from approximately 0.02–4.9 $g C m^{-2} month^{-1}$ in the study by Svensson et al. (1999) and from approximately 0.9–5.3 $g C m^{-2} month^{-1}$ in the study by Jackowicz-Korczyński et al. (2010). It was difficult for the model to catch peak values for most years (1974, 1995, 2006, and 2007) at this location (Fig. 5a, b). For another study (Granberg et al., 2001) carried out in a boreal mire in Sweden, however, the model simulated seasonal CH_4 emission variability with reasonable accuracy (Fig. 5c).

Mean emission rates of four different vegetation surfaces (hummocks, flarks, *Eriophorum* lawns, and *Carex* lawns) from a study by Saarnio et al. (1997) was calculated to make a comparison with modelled results from the current study (Fig. 5d). Modelled daily CH_4 emission rates agreed well with ranges of observed scatter points (Fig. 5d).

GMDD
6, 5423–5473, 2013

CH_4 flux from a study by Rinne et al. (2007) was measured using the eddy covariance technique. Gap filling data using linear interpolation in that study was adapted for the modelling test carried out in the current study. Variation in modelled CH_4 emissions was consistent with that observed before early July and after mid-September (Fig. 5e). During the period from early July to mid-September, there was a drop in observed emission rates (Fig. 5e). Modelled emission rates also diminished in July before once again increasing around mid-August. However, modelled emission rates showed higher values than observed emission rates during this period (Fig. 5e).

In a study by Panikov and Dedysh (2000), annual variation in CH_4 emissions was comparatively high, even during the same seasons. For example, emission rates in July ranged from 3.2 $g C m^{-2} month^{-1}$ (1997) to 10.8 $g C m^{-2} month^{-1}$ (1995) (Fig. 5f). The model simulated CH_4 emissions at this site reasonably well with the exception of those years that exhibited extremely high variation (e.g., 1993 and 1995) (Fig. 5f).

4.2.3 America

Observational data of the Fairbanks site (Fig. 6a) was obtained from The United States Trace Gas Network (TRAGNET) online database (http://www.nrel.colostate.edu/projects/tragnet/) described in a workshop reported by Ojima et al. (1992). Observational data provided in Fig. 6f (Sallie's fen) was obtained from the National Center for Ecological Analysis and Synthesis (NCEAS) data repository (Zhuang and Crill, 2008). The remaining observed data were digitized from corresponding citations (Fig. 6b–e) (Bartlett et al., 1989; Burke et al., 1988; Clement et al., 1995; Dise, 1993; Harriss et al., 1988; Shannon and White, 1994; Wickland et al., 2001). Although the model overestimated or underestimated emission rates for some peak values (e.g., Fig. 6a and f), Fig. 6 shows that general seasonal patterns of CH_4 emissions simulated by the model were consistent with observations.

For the site located in north central Minnesota, the mean emission rate was calculated based on observations carried out under different vegetation conditions from a study by Dise (1993). Simulated CH_4 emissions were slightly lower than that

GMDD
6, 5423–5473, 2013

of observed emissions for winter (Fig. 6b). Modelled results agreed better for 1991 static chamber data than for eddy correlation data (Fig. 6c). Observed CH_4 emissions collected from three individual flux chambers distributed approximately 10 m apart in a study by Shannon and White (1994) were compared to simulated CH_4 emissions on a daily scale between 1991–1993 (Fig. 6d). Although the model failed to capture the 1991 summer emission pulse, it performed well for both 1992 and 1993 (Fig. 6d).

For the site reported in a study by Wickland et al. (2001), the model again failed to capture peak emissions during the growing season in the first comparison year (1996), but it agreed quit well with observed data in the following two years (Fig. 6e).

For the Sallie's fen site (Zhuang and Crill, 2008), simulated seasonal and annual variation agreed well with an eight-year uninterrupted observation (Fig. 6f). However, the model failed to capture several peak values during the growing season at this site. The peak emission patterns were shown in most of the observational years and especially high in 1994 (Fig. 6f).

Studies carried out in the Florida Everglades have no precise geographical point location. Regional averaged modelling results around the Everglades National Park were used for comparison instead (Table 5). Variation in observations ranged from $3.0\,mg\,C\,m^{-2}\,day^{-1}$ to $481.5\,mg\,C\,m^{-2}\,day^{-1}$. However, the highest emission rate ($481.5\,mg\,C\,m^{-2}\,day^{-1}$) was measured in an open water site while rapid ebullition was observed on all sampling dates (Burke et al., 1988). This produced extremely high CH_4 flux at this particular site. Emissions ranged from $3.0\,mg\,C\,m^{-2}\,day^{-1}$ to $186.0\,mg\,C\,m^{-2}\,day^{-1}$ if excluding the open water site. Based on grid statistics, the simulated mean CH_4 emission for this area was approximately $60.0\,mg\,C\,m^{-2}\,day^{-1}$ with a variation of approximately $20.0\,mg\,C\,m^{-2}\,day^{-1}$. Modelled emission rate ranges were generally consistent with observed data (Table 5).

GMDD
6, 5423–5473, 2013

4.2.4 Canada

Figure 7a and b show CH_4 emission rate comparisons between model simulations and observed data obtained from the Boreal Ecosystem–Atmosphere Study (BOREAS), a large-scale international interdisciplinary experiment situated in the northern boreal forests of Canada (Sellers et al., 1997). Observed data were primarily collected from the Tower Flux (TF) science group and the Trace Gas Biogeochemistry science group from two study areas: the Southern Study Area (SSA) and the Northern Study Area (NSA) (http://daac.ornl.gov/BOREAS/bhs/BOREAS_Home.html). Only wetland data (SSA-fen and NSA-fen) was used for comparison on a daily scale in this study. Daily observed CH_4 emission rates provided in Fig. 7a and b were calculated based on sub-daily data of 10 sub-sites for SSA and four sub-sites for NSA (Fig. 7a and b). Magnitude of observed CH_4 emission rates for SSA was approximately twice that compared to NSA. For NSA, the mean CH_4 emission rate for 1996 was nearly twice that compared to 1994. These patterns indicate high temporal and spatial variation accompanied to CH_4 flux in these areas. For SSA, the model failed to capture the 1994 peak emission. There was an approximate one month delay for the simulated peak emission rate when compared to observed data from 1995. For NSA, observed scattering data points show that seasonal variation in CH_4 emissions was less clear compared to SSA. Moreover, NSA observations show a larger variance rang compared to SSA. The model overestimated 1994 CH_4 emissions while 1996 showed better performance. Nevertheless, the simulation was totally within the variance range of observations.

From a study by Pelletier et al. (2007), observed CH_4 emission rates measured on peatland covered by different vegetation types (excluding pools) was averaged for comparison. One extremely high observed outlier data point (higher by an approximate magnitude of 30 when compared to normal values) was rejected at site1 (Fig. 7c1). However, most observed points fell on simulated lines (Fig. 7c1–c3).

In a comparison with results reported by Moore et al. (2011), the model overestimated 2004 CH_4 emissions but underestimated those from 2006 (note: three

GMDD
6, 5423–5473, 2013

observed value points that were much greater than 0.3 g C m^{-2} day^{-1} in 2006 are not shown on the graph), but it agreed well with observations from 2005 and 2007 (Fig. 7d).

4.2.5 Southern Hemisphere

Several studies carried out in the Amazon Basin (Bartlett et al., 1990, 1988; Devol et al., 1988; Melack et al., 2004) and Australia (Boon, 1995) were selected for model testing in the Southern Hemisphere.

Since precise information on field site locations was unavailable for the Amazon Basin, a simple comparison of monthly mean CH_4 emissions was made between mean field observations and regional averaged modelled results (Table 6). Modelled monthly CH_4 emission rates were close to flooded forest emissions rates reported by Bartlett et al. (1990, 1988). Melack et al. (2004) reported that CH_4 emissions from the central Amazon Basin had a mean value of 6.8 Tg C yr^{-1}, based on remote sensing estimation. Total emissions for the same area where Melack et al. (2004) carried out their study was evaluated by the current study, based on regional simulations. Modelled annual total emissions were 6.32 Tg C yr^{-1}, which was close to the value (6.8) reported by Melack et al. (2004).

Additionally, a set of observed CH_4 emission data related to freshwater wetlands in south-eastern Australia was digitized from a study by Boon (1995) where field work was carried out over a 14 month period in 1993 and 1994. Seasonal and annual variation patterns for model simulations and observations stood in good agreement with each other (Fig. 8).

5 Discussion

Several process-based models have been developed to estimate CH_4 wetland emissions in recent years. With their own features and approaches in describing production, consumption, and transportation – three key CH_4 processes – some rely

GMDD
6, 5423–5473, 2013

more on empirical equations and some rely more on mechanisms to simulate such processes. Each model has advantages and disadvantages. Certain assumptions and equations from previous studies and models were adopted by this study to construct the CH_4 emissions model before being integrated into a DGVM (IBIS) model. Parameters relatively high in sensitivity were determined through sensitivity analysis. After which, the model was developed to simply and effectively capture patterns and track processes of CH_4 emissions from wetlands. Previous studies show that CH_4 production and oxidation were primarily dependent on temperature, which is controlled by Q10 values (Walter and Heimann, 2000; Walter et al., 2001b; Cao et al., 1996; Riley et al., 2011). Moreover, the release ratio of CH_4 to CO_2 was considered as the most important and influencing parameter for CH_4 emissions (Spahni et al., 2011; Wania et al., 2010). For sensitivity analysis, Wania et al. (2010) tested seven parameters using more than 2000 different parameter combinations; Riley et al. (2011) tested different parameters for CH_4 production, consumption, and transportation processes; Meng et al. (2012) tested eight parameters for sensitivity within certain possible ranges. For this study, only three parameters were selected (the release ratio of CH_4 to CO_2, Q10 for CH_4 production, and Q10 for CH_4 oxidation). After which, a series of sensitivity analysis was carried out for each parameter. Results show that Q10 for CH_4 production had a much higher sensitivity level than Q10 for CH_4 oxidation. Much stronger temperature dependence during production compared to oxidation was also reported in previous studies (Riley et al., 2011; Walter and Heimann, 2000; Walter et al., 2001b; Wania et al., 2010; Meng et al., 2012). The release ratio of CH_4 to CO_2 was highly sensitive to CH_4 emission processes and had direct impacts on CH_4 production. The studies that incorporated this parameter in CH_4 production also indicated that the release ratio of CH_4 to CO_2 was the parameter that most influenced CH_4 emissions, and the ratio varied with large ranges (Riley et al., 2011; Wania et al., 2010; Spahni et al., 2011; Meng et al., 2012). Based on sensitivity analysis, the release ratio of CH_4 to CO_2 and Q10 for CH_4 production – the two most important factors controlling

GMDD
6, 5423–5473, 2013

CH_4 emissions – were selected for parameter fitting in order to ascertain the best combination to test model performance and calibrate for individual sites.

Additionally, simulated results indicated that the sensitivity of Q10 in methane production increases as changes in Q10 values increase, while *r* (the release ratio of CH_4 to CO_2) remains at the same level of sensitivity regardless of change. Furthermore, sensitivity levels of each parameter showed seasonal pattern variations, indicating that model parameters are much more sensitive during winter than summer. This suggests that CH_4 emissions are more sensitive during winter as temperatures change.

As shown in Fig. 6d–f, some simulated results failed to capture peak observational CH_4 emission values during the growing season, suggesting that CH_4 emission pulse underestimation may be partly due to external environmental triggers not included in the model nor CH_4 contribution from microbial mat systems during summer (Tian et al., 2010; Shoemaker and Schrag, 2010). To date, mechanisms that drive peak CH_4 emission flux is still unknown, even though the phenomenon has been observed in numerous studies (Tian et al., 2010). Based on comparisons, this study also detected some simulated peak emission values not reported in observations (e.g., Figs. 5c and e, 6a and 7c1–c3). One possible explanation could be the low sampling frequency typical of field work. Although some comparisons were carried out between simulations and observations using the high frequency eddy covariance technique rather than low frequency flux chambers, the footprint associated with eddy flux estimation depends on wind properties, boundary layers, surface roughness, etc. (Riley et al., 2011). Nevertheless, the model was able to capture seasonal CH_4 emission variation patterns. For example, a drop in observed emission rates was detected in a study by Rinne et al. (2007) during early July to mid-September (Fig. 5e). This suggests that CH_4 emissions were independent with the peat temperature during this period. It also suggests the major reason for this emissions drop may be that the methanogenic microbe population exceeded growth in available substrates (Rinne

GMDD
6, 5423–5473, 2013

et al., 2007). A drop pattern was also found in model simulation during the same period, though emission magnitude was slightly higher than that of observed (Fig. 5e).

The differences in scale between simulation and site observations may be another important reason explaining differences between model simulations and observations. At each site, global scale climate dataset (CRU-TS 3.1 Climate Database) was used for simulations. The climate dataset cannot reflect the details of the daily or seasonal variation in temporal respect, and also can not reflect the specified site characteristics with an average value in a large grid. Local climates may differ significantly from grid climates, especially in regions of high relief (Wania et al., 2010). Biases may be added to simulations of net primary productivity (NPP), heterotrophic respiration, soil water, and thermal processes, which are important parameters for CH_4 production. Subsequently, it is difficult for the model to capture full emission patterns at site levels using relatively coarse climate forcing, sometimes with a time-lag (e.g. the simulation at BOREAS SSA in 1995, Fig. 7a). Site level topographic heterogeneity is difficult to replicate, which is also a reason for model simulation and observation disagreement.

Uncertainties in the field observations should also be taken into account in comparisons. In many studies, for example, observations taken in the first year typically differ in subsequent years (e.g., Fig. 6a, d and f). This may be due to conditions where observational systems are unstable during initial setup. Larger differences are exhibited in the first year between simulations and observations. Differences between different observations for the same site also indicate uncertainties in observations (e.g., Fig. 4a and b), which may be the result of the different methods used for observations or differences in micrometeorology or microtopography used in different measurements. Bias in comparisons is therefore inevitable.

It is important to note that parameter values analyzed in this study (the release ratio of CH_4 to CO_2 and Q10 for CH_4 production) were different for different sites or different regions. For the parameter fitting process, we tried to find the best site-specific parameters and to show how well the model can perform at local site conditions. This will continue to be an important issue in regional and global scale

GMDD
6, 5423–5473, 2013

simulation development. Using different parameter sets for different locations or using an overall uniform parameter set (e.g., average values for all sites) for regional or global simulations should be considered. Collecting the largest possible observed CH_4 emissions dataset from different geographic locations and different wetland types will produce the best parameter set for use in parameter fitting for each location or type. After which, a spatial distribution layer or database for highly sensitive parameters for regional or global modelling can be constructed.

Although water tables are essential in CH_4 production, consumption, and transportation processes, it was difficult to obtain observed water table data to test the performance of the water table module for each site discussed in this study. More data collection through means of literature reviews or field measurements is needed to test simulation performance and parameterization of the water table module.

6 Conclusions

This study introduces the successful integration of a CH_4 biogeochemistry module incorporating CH_4 production, oxidation, and transportation processes into an existing DGVM (IBIS), which is also part of the most recent development of the TRIPLEX-GHG model framework. Factors controlling CH_4 emission processes, such as soil temperature, redox potential, and pH were specified into the model. A water table module was also integrated into DGVM to improve hydrological processes for wetland simulation. Sensitivity analysis indicates that the release ratio of CH_4 to CO_2 and Q10 for CH_4 production are two major controlling factors in CH_4 emission modelling. Moreover, values of these two parameters are spatially heterogeneous. Model tests were carried out in 19 sites across different geographical regions throughout the world. Although the model sometimes failed to simulate daily details or the emission pulse, it was always successful in capturing patterns in temporal variation. Results suggest that the model can be applied to different wetlands under varying conditions. It would also be applicable on a global scale. Some parameters in the modeling

GMDD
6, 5423–5473, 2013

are site-specific, which means that more process-based approaches are needed in methane biogeochemistry modeling instead of experimental assumptions, especially in the methane emission estimation at regional or global scale.

Acknowledgements. This study was funded by the National Basic Research Program of China (2013CB956602), the National Natural Science Foundation of China (41201079), the Start-up Funds (Z111021203) and Basic Research Funds (Z109021204) of Northwest A&F University, the Specialized Research Fund for the Doctoral Program of Higher Education of China (20120204120007), and the Natural Sciences and Engineering Research Council of Canada Discovery Grant.

References

Arneth, A., Sitch, S., Bondeau, A., Butterbach-Bahl, K., Foster, P., Gedney, N., de Noblet-Ducoudré, N., Prentice, I. C., Sanderson, M., Thonicke, K., Wania, R., and Zaehle, S.: From biota to chemistry and climate: towards a comprehensive description of trace gas exchange between the biosphere and atmosphere, Biogeosciences, 7, 121–149, doi:10.5194/bg-7-121-2010, 2010.

Bartlett, D. S., Bartlett, K. B., Hartman, J. M., Harriss, R. C., Sebacher, D. I., Pelletier-Travis, R., Dow, D. D., and Brannon, D. P.: Methane emissions from the Florida Everglades: patterns of variability in a regional wetland ecosystem, Global Biogeochem. Cy., 3, 363–374, doi:10.1029/GB003i004p00363, 1989.

Bartlett, K. B., Crill, P. M., Sebacher, D. I., Harriss, R. C., Wilson, J. O., and Melack, J. M.: Methane flux from the central Amazonian Floodplain, J. Geophys. Res., 93, 1571–1582, doi:10.1029/JD093iD02p01571, 1988.

Bartlett, K. B., Crill, P. M., Bonassi, J. A., Richey, J. E., and Harriss, R. C.: Methane flux from the Amazon River floodplain: emissions during rising water, J. Geophys. Res., 95, 16773–16788, 1990.

Boon, P. I.: Methanogenesis in the sediments of an Australian freshwater wetland: comparison with aerobic decay, and factors controlling methanogenesis, Fems Microbiol. Ecol., 18, 175–190, doi:10.1016/0168-6496(95)00053-5, 1995.

GMDD

6, 5423–5473, 2013

Burke Jr., R. A., Barber, T. R., and Sackett, W. M.: Methane flux and stable hydrogen and carbon isotope composition of sedimentary methane from the Florida Everglades, Global Biogeochem. Cy., 2, 329–340, doi:10.1029/GB002i004p00329, 1988.

Cao, M., Dent, J. B., and Heal, O. W.: Modeling methane emissions from rice paddies, Global Biogeochem. Cy., 9, 183–195, doi:10.1029/94gb03231, 1995.

Cao, M., Marshall, S., and Gregson, K.: Global carbon exchange and methane emissions from natural wetlands: application of a process-based model, J. Geophys. Res.-Atmos., 101, 14399–14414, 1996.

Chen, H., Yao, S., Wu, N., Wang, Y., Luo, P., Tian, J., Gao, Y., and Sun, G.: Determinants influencing seasonal variations of methane emissions from alpine wetlands in Zoige Plateau and their implications, J. Geophys. Res., 113, D12303, doi:10.1029/2006jd008072, 2008.

Chen, H., Zhu, Q., Peng, C., Wu, N., Wang, Y., Fang, X., Jiang, H., Xiang, W., Chang, J., Deng, X., and Yu, G.: Methane emissions from rice paddies natural wetlands, and lakes in China: synthesis and new estimate, Glob. Change Biol., 19, 19–32, doi:10.1111/gcb.12034, 2013.

Chen, Y. H. and Prinn, R. G.: Atmospheric modeling of high- and low-frequency methane observations: Importance of interannually varying transport, J. Geophys. Res.-Atmos., 110, D10303, doi:10.1029/2004jd005542, 2005.

Clement, R. J., Verma, S. B., and Verry, E. S.: Relating chamber measurements to eddy-correlation measurements of methane flux, J. Geophys. Res.-Atmos., 100, 21047–21056, 1995.

Cramer, W., Bondeau, A., Woodward, F. I., Prentice, I. C., Betts, R. A., Brovkin, V., Cox, P. M., Fisher, V., Foley, J. A., Friend, A. D., Kucharik, C., Lomas, M. R., Ramankutty, N., Sitch, S., Smith, B., White, A., and Young-Molling, C.: Global response of terrestrial ecosystem structure and function to CO_2 and climate change: results from six dynamic global vegetation models, Glob. Change Biol., 7, 357–373, 2001.

Cui, B.: Estimation of CH_4 emission from Sanjiang plain, Sci. Geogr. Sin., 17, 93–95, 1997 (in Chinese with English abstract).

Denman, K. L., Brasseur, G., Chidthaisong, A., Ciais, P., Cox, P. M., Dickinson, R. E., Hauglustaine, D., Heinze, C., Holland, E., Jacob, D., Lohmann, U., Ramachandran, S., Dias, P. L. D. S., Wofsy, S. C., and Zhang, X.: Couplings between changes in the climate system and biogeochemistry, in: Climate Change 2007: The Physical Science Basis, Contribution of Working Group I to the Fourth Assessment Report of the Intergovernmental

GMDD
6, 5423–5473, 2013

Panel on Climate Change, edited by: Solomon, S., Qin, D., Manning, M., Chen, Z., Marquis, M., Averyt, K. B., Tignor, M., and Miller, H. L., Cambridge University Press, Cambridge, UK and New York, USA, 2007.
Devol, A. H., Richey, J. E., Clark, W. A., King, S. L., and Martinelli, L. A.: Methane emissions to the troposphere from the Amazon floodplain, J. Geophys. Res., 93, 1583–1592, 1988.
Ding, W., Cai, Z., and Wang, D.: Preliminary budget of methane emissions from natural wetlands in China, Atmos. Environ., 38, 751–759, doi:10.1016/j.atmosenv.2003.10.016, 2004.
Dise, N. B.: Winter fluxes of methane from Minnesota Peatlands, Biogeochemistry, 17, 71–83, 1992.
Dise, N. B.: Methane emission from Minnesota Peatlands – spatial and seasonal variability, Global Biogeochem. Cy., 7, 123–142, 1993.
Dunfield, P., Knowles, R., Dumont, R., and Moore, T. R.: Methane production and consumption in temperate and subarctic peat soils: response to temperature and pH, Soil Biol. Biochem., 25, 321–326, 1993.
Enting, I., Heimann, M., and Wigley, T.: Future emissions and concentrations of carbon dioxide: key ocean/atmosphere/land analyses, CSIRO Division of Atmospheric Research, Technical Paper No. 31, CSIRO, Australia, 1994.
Fiedler, S. and Sommer, M.: Methane emissions, groundwater levels and redox potentials of common wetland soils in a temperate-humid climate, Global Biogeochem. Cy., 14, 1081–1093, doi:10.1029/1999gb001255, 2000.
Foley, J. A., Colin, P. I., Ramankutty, N., Levis, S., Pollard, D., Sitch, S., and Haxeltine, A.: An integrated biosphere model of land surface processes, terrestrial carbon balance, and vegetation dynamics, Global Biogeochem. Cy., 10, 603–628, 1996.
Gedney, N., Cox, P. M., and Huntingford, C.: Climate feedback from wetland methane emissions, Geophys. Res. Lett., 31, L20503, doi:10.1029/2004gl020919, 2004.
Granberg, G., Grip, H., Ottosson Löfvenius, M., Sundh, I., Svensson, B. H., and Nilsson, M.: A simple model for simulation of water content, soil frost, and soil temperatures in boreal mixed mires, Water Resour. Res., 35, 3771–3782, doi:10.1029/1999wr900216, 1999.
Granberg, G., Ottosson-Lofvenius, M., Grip, H., Sundh, I., and Nilsson, M.: Effect of climatic variability from 1980 to 1997 on simulated methane emission from a boreal mixed mire in northern Sweden, Global Biogeochem. Cy., 15, 977–991, 2001.

GMDD
6, 5423–5473, 2013

Hao, Q., Wang, Y., Song, C., Liu, G., Wang, Y., and Wang, M.: Study of CH_4 emission from wetlands in Sanjiang Plain, J. Soil Water Conservat., 18, 194–199, 2004 (in Chinese with English abstract).

Harriss, R. C., Sebacher, D. I., Bartlett, K. B., Bartlett, D. S., and Crill, P. M.: Sources of atmospheric methane in the south Florida environment, Global Biogeochem. Cy., 2, 231–243, doi:10.1029/GB002i003p00231, 1988.

Huang, Y., Sun, W. J., Zhang, W., Yu, Y. Q., Su, Y. H., and Song, C. C.: marshland conversion to cropland in northeast China from 1950 to 2000 reduced the greenhouse effect, Glob. Change Biol., 16, 680–695, doi:10.1111/j.1365-2486.2009.01976.x, 2010.

Ito, A. and Inatomi, M.: Use of a process-based model for assessing the methane budgets of global terrestrial ecosystems and evaluation of uncertainty, Biogeosciences, 9, 759–773, doi:10.5194/bg-9-759-2012, 2012.

Jackowicz-Korczyński, M., Christensen, T. R., Bäckstrand, K., Crill, P., Friborg, T., Mastepanov, M., and Ström, L.: Annual cycle of methane emission from a subarctic peatland, J. Geophys. Res., 115, G02009, doi:10.1029/2008jg000913, 2010.

Keeling, C. D., Piper, S. C., Bacastow, R. B., Wahlen, M., Whorf, T. P., Heimann, M., and Meijer, H. A.: Atmospheric CO_2 and $^{13}CO_2$ exchange with the terrestrial biosphere and oceans from 1978 to 2000: observations and carbon cycle implications, in: A History of Atmospheric CO_2 and Its Effects on Plants Animals and Ecosystems, edited by: Ehleringer, J. R., Cerling, T. E., and Dearing, M. D., Springer Verlag, New York, 83–113, 2005.

Kucharik, C. J., Foley, J. A., Delire, C., Fisher, V. A., Coe, M. T., Lenters, J. D., Young-Molling, C., and Ramankutty, N.: Testing the performance of a dynamic global ecosystem model: water balance, carbon balance, and vegetation structure, Global Biogeochem. Cy., 14, 795–825, 2000.

Kucharik, C. J., Barford, C. C., El Maayar, M., Wofsy, S. C., Monson, R. K., and Baldocchi, D. D.: A multiyear evaluation of a Dynamic Global Vegetation Model at three AmeriFlux forest sites: Vegetation structure, phenology, soil temperature, and CO_2 and H_2O vapor exchange, Ecol. Model., 196, 1–31, doi:10.1016/j.ecolmodel.2005.11.031, 2006.

Lenhart, T., Eckhardt, K., Fohrer, N., and Frede, H.-G.: Comparison of two different approaches of sensitivity analysis, Phys. Chem. Earth, 27, 645–654, 2002.

Li, C. S.: Modeling trace gas emissions from agricultural ecosystems, Nutr. Cycl. Agroecosys., 58, 259–276, doi:10.1023/a:1009859006242, 2000.

GMDD
6, 5423–5473, 2013

Melack, J. M., Hess, L. L., Gastil, M., Forsberg, B. R., Hamilton, S. K., Lima, I. B. T., and Novo, E. M. L. M.: Regionalization of methane emissions in the Amazon Basin with microwave remote sensing, Glob. Change Biol., 10, 530–544, doi:10.1111/j.1365-2486.2004.00763.x, 2004.

Melloh, R. A. and Crill, P. M.: Winter methane dynamics in a temperate peatland, Global Biogeochem. Cy., 10, 247–254, 1996.

Melton, J. R., Wania, R., Hodson, E. L., Poulter, B., Ringeval, B., Spahni, R., Bohn, T., Avis, C. A., Beerling, D. J., Chen, G., Eliseev, A. V., Denisov, S. N., Hopcroft, P. O., Lettenmaier, D. P., Riley, W. J., Singarayer, J. S., Subin, Z. M., Tian, H., Zürcher, S., Brovkin, V., van Bodegom, P. M., Kleinen, T., Yu, Z. C., and Kaplan, J. O.: Present state of global wetland extent and wetland methane modelling: conclusions from a model inter-comparison project (WETCHIMP), Biogeosciences, 10, 753–788, doi:10.5194/bg-10-753-2013, 2013.

Meng, L., Hess, P. G. M., Mahowald, N. M., Yavitt, J. B., Riley, W. J., Subin, Z. M., Lawrence, D. M., Swenson, S. C., Jauhiainen, J., and Fuka, D. R.: Sensitivity of wetland methane emissions to model assumptions: application and model testing against site observations, Biogeosciences, 9, 2793–2819, doi:10.5194/bg-9-2793-2012, 2012.

Moore, T. R. and Knowles, R.: Methane emissions from fen, bog and swamp peatlands in Quebec, Biogeochemistry, 11, 45–61, 1990.

Moore, T. R., De Young, A., Bubier, J. L., Humphreys, E. R., Lafleur, P. M., and Roulet, N. T.: A multi-year record of methane flux at the Mer Bleue Bog, Southern Canada, Ecosystems, 14, 646–657, doi:10.1007/s10021-011-9435-9, 2011.

Nouchi, I., Hosono, T., Aoki, K., and Minami, K.: Seasonal-variation in methane flux from rice paddies associated with methane concentration in soil-water, rice biomass and temperature, and its modeling, Plant Soil, 161, 195–208, 1994.

Ojima, D. S., Holland, E. A., Melillo, J. M., Mosier, A. R., and Robertson, G. P.: TRAGNET workshop report: building a US trace gas network, Pingree Park, Colorado, USA, 1992.

Panikov, N. S. and Dedysh, S. N.: Cold season CH_4 and CO_2 emission from boreal peat bogs (West Siberia): winter fluxes and thaw activation dynamics, Global Biogeochem. Cy., 14, 1071–1080, 2000.

Pelletier, L., Moore, T. R., Roulet, N. T., Garneau, M., and Beaulieu-Audy, V.: Methane fluxes from three peatlands in the La Grande Riviere watershed, James Bay lowland, Canada, J. Geophys. Res.-Biogeo., 112, G01018, doi:10.1029/2006jg000216, 2007.

GMDD
6, 5423–5473, 2013

Peng, C., Liu, J., Dang, Q., Apps, M. J., and Jiang, H.: TRIPLEX: a generic hybrid model for predicting forest growth and carbon and nitrogen dynamics, Ecol. Model., 153, 109–130, doi:10.1016/s0304-3800(01)00505-1, 2002.

Peng, C. H., Zhu, Q. A., and Chen, H.: Integrating greenhouse gas emission processes into a dynamic global vegetation model of TRIPLEX-GHG, EGU General Assembly, Vienna, Austria, EGU2013-1486, April 2013.

Petrescu, A. M. R., van Beek, L. P. H., van Huissteden, J., Prigent, C., Sachs, T., Corradi, C. A. R., Parmentier, F. J. W., and Dolman, A. J.: Modeling regional to global CH_4 emissions of boreal and arctic wetlands, Global Biogeochem. Cy., 24, GB4009, doi:10.1029/2009gb003610, 2010.

Prentice, I. C., Webb, R. S., Ter-Mikhaelian, M. T., Solomon, A. M., Smith, T. M., Pitovranov, S. E., Nikolov, N. T., Minin, A. A., Leemans, R., Lavorel, S., Korzukhin, M. D., Hrabovszky, J. P., Helmisaari, H. O., Harrison, S. P., Emanuel, W. R., and Bonan, G. B.: Developing a global vegetation dynamics model: results of an IIASA summer workshop, 52 pp., Laxenburg, Austria, August 1989.

Riley, W. J., Subin, Z. M., Lawrence, D. M., Swenson, S. C., Torn, M. S., Meng, L., Mahowald, N. M., and Hess, P.: Barriers to predicting changes in global terrestrial methane fluxes: analyses using CLM4Me, a methane biogeochemistry model integrated in CESM, Biogeosciences, 8, 1925–1953, doi:10.5194/bg-8-1925-2011, 2011.

Rinne, J., Riutta, T., Pihlatie, M., Aurela, M., Haapanala, S., Tuovinen, J. P., Tuittila, E. S., and Vesala, T.: Annual cycle of methane emission from a boreal fen measured by the eddy covariance technique, Tellus B, 59, 449–457, doi:10.1111/j.1600-0889.2007.00261.x, 2007.

Saarnio, S., Alm, J., Silvola, J., Lohila, A., Nykänen, H., and Martikainen, P. J.: Seasonal variation in CH_4 emissions and production and oxidation potentials at microsites on an oligotrophic pine fen, Oecologia, 110, 414–422, doi:10.1007/s004420050176, 1997.

Sass, R. L., Fisher, F. M., Harcombe, P. A., and Turner, F. T.: Methane production and emission in a Texas rice field, Global Biogeochem. Cy., 4, 47–68, doi:10.1029/GB004i001p00047, 1990.

Segers, R.: Methane production and methane consumption: a review of processes underlying wetland methane fluxes, Biogeochemistry, 41, 23–51, 1998.

Segers, R. and Kengen, S. W. M.: Methane production as a function of anaerobic carbon mineralization: a process model, Soil Biol. Biochem., 30, 1107–1117, 1998.

GMDD
6, 5423–5473, 2013

Sellers, P. J., Hall, F. G., Kelly, R. D., Black, A., Baldocchi, D., Berry, J., Ryan, M., Ranson, K. J., Crill, P. M., Lettenmaier, D. P., Margolis, H., Cihlar, J., Newcomer, J., Fitzjarrald, D., Jarvis, P. G., Gower, S. T., Halliwell, D., Williams, D., Goodison, B., Wickland, D. E., and Guertin, F. E.: BOREAS in 1997: experiment overview, scientific results, and future directions, J. Geophys. Res.-Atmos., 102, 28731–28769, 1997.

Shannon, R. D. and White, J. R.: A three-year study of controls on methane emissions from two Michigan Peatlands, Biogeochemistry, 27, 35–60, 1994.

Shannon, R. D., White, J. R., Lawson, J. E., and Gilmour, B. S.: Methane efflux from emergent vegetation in peatlands, J. Ecol., 84, 239–246, 1996.

Shindell, D. T., Walter, B. P., and Faluvegi, G.: Impacts of climate change on methane emissions from wetlands, Geophys. Res. Lett., 31, L21202, doi:10.1029/2004gl021009, 2004.

Shoemaker, J. K. and Schrag, D. P.: Subsurface characterization of methane production and oxidation from a New Hampshire wetland, Geobiology, 8, 234–243, doi:10.1111/j.1472-4669.2010.00239.x, 2010.

Song, C., Xu, X., Tian, H., and Wang, Y.: Ecosystem–atmosphere exchange of CH_4 and N_2O and ecosystem respiration in wetlands in the Sanjiang Plain, Northeastern China, Glob. Change Biol., 15, 692–705, doi:10.1111/j.1365-2486.2008.01821.x, 2009.

Spahni, R., Wania, R., Neef, L., van Weele, M., Pison, I., Bousquet, P., Frankenberg, C., Foster, P. N., Joos, F., Prentice, I. C., and van Velthoven, P.: Constraining global methane emissions and uptake by ecosystems, Biogeosciences, 8, 1643–1665, doi:10.5194/bg-8-1643-2011, 2011.

Strom, L., Mastepanov, M., and Christensen, T. R.: Species-specific effects of vascular plants on carbon turnover and methane emissions from wetlands, Biogeochemistry, 75, 65–82, 2005.

Svensson, B. H., Christensen, T. R., Johansson, E., and Oquist, M.: Interdecadal changes in CO_2 and CH_4 fluxes of a subarctic mire: Stordalen revisited after 20 yr, Oikos, 85, 22–30, 1999.

Tian, H., Xu, X., Liu, M., Ren, W., Zhang, C., Chen, G., and Lu, C.: Spatial and temporal patterns of CH_4 and N_2O fluxes in terrestrial ecosystems of North America during 1979–2008: application of a global biogeochemistry model, Biogeosciences, 7, 2673–2694, doi:10.5194/bg-7-2673-2010, 2010.

Valentine, D. W., Holland, E. A., and Schinel, D. S.: Ecosystem and physical controls over methane production in northern wetlands, J. Geophys. Res., 99, 1563–1571, 1994.

GMDD
6, 5423–5473, 2013

Van Ham, J., Baede, A. P. M., Meyer, L. A., and Ybema, R.: Non-CO_2 greenhouse gases: scientific understanding, control and implementation, Kluwer Academic Pub., Dordrecht, the Netherlands, 2000.
van Huissteden, J., van den Bos, R., and Alvarez, I. M.: Modelling the effect of water-table management on CO_2 and CH_4 fluxes from peat soils, Neth. J. Geosci., 85, 3–18, 2006.
Walter, B. P. and Heimann, M.: A process-based, climate-sensitive model to derive methane emissions from natural wetlands: application to five wetland sites, sensitivity to model parameters, and climate, Global Biogeochem. Cy., 14, 745–765, doi:10.1029/1999gb001204, 2000.
Walter, B. P., Heimann, M., and Matthews, E.: Modeling modern methane emissions from natural wetlands 1. Model description and results, J. Geophys. Res., 106, 34189–34206, doi:10.1029/2001jd900165, 2001a.
Walter, B. P., Heimann, M., and Matthews, E.: Modeling modern methane emissions from natural wetlands 2. Interannual variations 1982–1993, J. Geophys. Res., 106, 34207–34219, doi:10.1029/2001jd900164, 2001b.
Wang, D., Lu, X., Ding, W., Cai, Z., Gao, J., and Yang, F.: Methane emission from marshes in Zoige Plateau, Adv. Earth Sci., 17, 877–880, 2002a.
Wang, D., Lu, X., Ding, W., Cai, Z., and Wang, Y.: Comparison of methane emission from marsh and paddy field in Sanjiang Plain, Sci. Geogr. Sin., 22, 500–503, 2002b (in Chinese with English abstract).
Wang, Y. P., Law, R. M., and Pak, B.: A global model of carbon, nitrogen and phosphorus cycles for the terrestrial biosphere, Biogeosciences, 7, 2261–2282, doi:10.5194/bg-7-2261-2010, 2010.
Wang, Z. P., Delaune, R. D., Masscheleyn, P. H., and Patrick, W. H.: Soil redox and Ph effects on methane production in a flooded rice soil, Soil Sci. Soc. Am. J., 57, 382–385, 1993.
Wania, R., Ross, I., and Prentice, I. C.: Integrating peatlands and permafrost into a dynamic global vegetation model: 2. Evaluation and sensitivity of vegetation and carbon cycle processes, Global Biogeochem. Cy., 23, GB3015, doi:10.1029/2008gb003413, 2009a.
Wania, R., Ross, I., and Prentice, I. C.: Integrating peatlands and permafrost into a dynamic global vegetation model: 1. Evaluation and sensitivity of physical land surface processes, Global Biogeochem Cy., 23, GB3014, doi:10.1029/2008gb003412, 2009b.

GMDD
6, 5423–5473, 2013

Wania, R., Ross, I., and Prentice, I. C.: Implementation and evaluation of a new methane model within a dynamic global vegetation model: LPJ-WHyMe v1.3.1, Geosci. Model Dev., 3, 565–584, doi:10.5194/gmd-3-565-2010, 2010.

Wania, R., Melton, J. R., Hodson, E. L., Poulter, B., Ringeval, B., Spahni, R., Bohn, T., Avis, C. A., Chen, G., Eliseev, A. V., Hopcroft, P. O., Riley, W. J., Subin, Z. M., Tian, H., van Bodegom, P. M., Kleinen, T., Yu, Z. C., Singarayer, J. S., Zürcher, S., Lettenmaier, D. P., Beerling, D. J., Denisov, S. N., Prigent, C., Papa, F., and Kaplan, J. O.: Present state of global wetland extent and wetland methane modelling: methodology of a model inter-comparison project (WETCHIMP), Geosci. Model Dev., 6, 617–641, doi:10.5194/gmd-6-617-2013, 2013.

Weiss, R., Shurpali, N. J., Sallantaus, T., Laiho, R., Laine, J., and Alm, J.: Simulation of water table level and peat temperatures in boreal peatlands, Ecol. Model., 192, 441–456, doi:10.1016/j.ecolmodel.2005.07.016, 2006.

Westermann, P.: Temperature regulation of methanogenesis in wetlands, Chemosphere, 26, 321–328, 1993.

Whalen, S. C. and Reeburgh, W. S.: Interannual variations in tundra methane emission: a 4-year time series at fixed sites, Global Biogeochem. Cy., 6, 139–159, doi:10.1029/92gb00430, 1992.

Whiting, G. J. and Chanton, J. P.: Primary production control of methane emission from wetlands, Nature, 364, 794–795, 1993.

Wickland, K. P., Striegl, R. G., Mast, M. A., and Clow, D. W.: Interannual variation of soil respiration in two New England forests, Global Biogeochem. Cy., 15, 321–335, doi:10.1029/2000gb001325, 2001.

Yang, J., Liu, J., Wang, J., Yu, J., Sun, Z., and Li, X.: Emissions of CH_4 and N_2O from a wetland in the Sanjiang plain, J. Plant Ecol., 30, 432–440, 2006 (in Chinese with English abstract).

Zhang, Y., Li, C., Trettin, C. C., Li, H., and Sun, G.: An integrated model of soil, hydrology, and vegetation for carbon dynamics in wetland ecosystems, Global Biogeochem. Cy., 16, 1061, doi:10.1029/2001GB001838, 2002.

Zhuang, Q., Melillo, J. M., Kicklighter, D. W., Prinn, R. G., McGuire, A. D., Steudler, P. A., Felzer, B. S., and Hu, S.: Methane fluxes between terrestrial ecosystems and 30 the atmosphere at northern high latitudes during the past century: a retrospective analysis with a process-based biogeochemistry model, Global Biogeochem. Cy., 18,, GB3010, doi:10.1029/2004GB002239, 2004.

GMDD
6, 5423–5473, 2013

Table 1. List of collected sites for model parameter fitting and calibration.

ID	Sites	Location	Latitude	Longitude	Type	Time	Method	Reference
1	Sanjiang plain	China	47°35′ N	133°31′ E	marshland	2002 ~ 2005	open-bottom chamber	Huang et al. (2010)
					natural freshwater wetland	2002 ~ 2005	dark chamber and gas chromatography techniques	Song et al. (2009)
					marshland	2001	static chamber	Wang et al. (2002)
					marshland	1995 ~ 1996	static chamber	Cui et al. (1997)
					freshwater marsh	2001 ~ 2002	open-ended plexiglass chambers	Ding et al. (2004)
					marshland	2003	static chamber	Yang et al. (2006)
					marshland	2002	static chamber	Hao et al. (2004)
					freshwater marshes	2004 ~ 2005	static chamber	Zhang et al. (2007)
2	Qinghai-Tibet	China	32°47′ N	102°32′ E	peatland	2001	static chamber	Wang et al. (2002)
					peatland	2001 ~ 2002	open-ended plexiglass chambers	Ding et al. (2004)
		China	33°56′ N	102°52′ E	peatland	2005 ~ 2006	static chamber	Chen et al. (2008)
3	Stordalen	Sweden	68°20′ N	19°03′ E	subarctic mire	1974/94/95	static chamber	Svensson et al. (1999)
						2006 ~ 2007	automatic chamber	Jackowicz-Korczynski et al. (2010)
4	Degero Stormyr	Sweden	64°11′ N	19°33′ E	boreal mire, fen	1995 ~ 1997	static chamber	Grandberg et al. (2001)
5	Salmisuo mire	Finland	62°47′ N	30°56′ E	pine fen	1993	static chamber	Saarnio et al. (1997)
6	Ruovesi	Finland	61°50′ N	24°12′ E	boreal fen	2005	eddy covarance technique	Rinne et al. (2007)
7	Plotnikovo West Siberia	Russia	57°00′ N	82°00′ E	ombrotrophic bogs	Jul 1993–1997	static chamber	Panikov et al. (2000)
8	Florida	USA	25°00′ N	81°00′ W	everglade	Jan ~ Feb (1984); Dec,1985	portable gas filter correlation (GFC) measurement system	Bartlett et al. (1989)
			South Florida		everglade	Jun, Nov 1986; Mar, Aug 1987	static chamber	Burke et al. (1988)
			South Florida		everglade	1980 (1982); 1985	gas filter correlation infrared absorption analyzer integrated with an open bottom chamber	Harriss et al. (1988)
9	Fairbanks Alaska	USA	64°48′ N	147°42′ W	wetland	1987 ~ 1990	static chamber	Ojima et al. (1992)
10	Minnesota	USA	47°32′ N	93°28′ W	peatland	1988 ~ 1990	static chamber	Dise et al. (1993)
						1991 ~ 1992	eddy correlation flux measurement and chamber flux measurement	Clement et al. (1995)
11	Michigan	USA	42°27′ N	84°01′ W	peatland, buck hollow bog	1991 ~ 1993	static chamber	Shannon et al. (1994)
12	Sallies Fen	USA	43°12.5′ N	71°3.5′ W	fen	1994 ~ 2001	static chamber	Zhuang et al. (2008)
13	Loch Vale, Colorado	USA	40°17′ N	105°39′ W	subalpine wetland	1996 ~ 1998	closed chamber	Wickland et al. (2001)
14	BOREAS SSA	Canada	53°48′ N	104°37′ W	peatland, fen	1994 ~ 1995	eddy flux tower and static chamber	Sellers et al. (1997)
15	BOREAS NSA	Canada	55°55′ N	98°25′ W	peatland, fen	1994/96	static chamber	Sellers et al. (1997)
16	Quebec	Canada	53°54′ N	78°46′ W	peatland	2003	static chamber	Pelletier et al. (2007)
			53°38′ N	77°43′ W	peatland	2003	static chamber	
			53°34′ N	76°08′ W	peatland	2003	static chamber	
17	Mer Bleue	Canada	45°41′ N	75°48′ W	peatland, bog	2004 ~ 2007	static chamber	Moore et al. (2011)
18	Ryans 1 Billagong	Australia	36°07′ S	146°58′ E	freshwater wetland	Apr 1993 ~ May 1994	static chamber	Boon et al. (1995)
19	Amazon	Brazil	Amazon Basin		flooded plain	1979 ~ 1987	satellite inverse	Melack et al. (2004)
						Jul ~ Aug 1985	static chamber	Devole et al. (1988)
						18 Jul ~ 2 Sep 1985	static chamber and gas filter correlation	Bartlett et al. (1988)
						Apr ~ May 1987	static chamber and gas filter correlation	Bartlett et al. (1990)

GMDD
6, 5423–5473, 2013

Table 2. List of major parameters in CH_4 production, oxidation, and transportation.

Process	Parameters	Values	Unit	Description	References
Methane production	T_{max}	45	°C	highest temperature for methane production	This study
	T_{opt}	25	°C	optimum temperature for methane production	This study
	pH_{high}	9	–	highest pH for methane production	Cao et al. (1996), Zhang et al. (2002), Zhuang et al. (2004)
	pH_{low}	4	–	lowest pH for methane production	Cao et al. (1996), Zhang et al. (2002), Zhuang et al. (2004)
	pH_{opt}	7	–	optimum pH for methane production	Cao et al. (1996), Zhang et al. (2002), Zhuang et al. (2004)
	r	0.1 ~ 0.4	–	ratio of CH_4 and CO_2	Wania et al. (2010), Zhang et al. (2002)
	Q10	1.7 ~ 16	–	Q10 for methane production	Dunfield et al. (1993), Walter et al. (2000)
Methane oxidation	K_{CH_4}	5	μmol	Michaelis–Menten coefficients	Walter et al. (2000), Zhang et al. (2002)
	Q10	1.4 ~ 2.4	–	Q10 for methane oxidation	Meng et al. (2012), Watter et al. (2000), Zhang et al. (2002), Seger et al. (1998)
Methane transportation	f_{tort}	0.66	–	tortuousity coefficient	Walter (2000)
	D_a	0.2	$cm^2 s^{-1}$	molecular diffusion coefficients of methane in the air	Walter et al. (2000)
	D_w	0.00002	$cm^2 s^{-1}$	molecular diffusion coefficients of methane in the water	Walter et al. (2000)
	f_{rhi}	0.5	–	factor of rhizospheric oxidation	Wania et al. (2010), Zhang et al. (2002)

GMDD
6, 5423–5473, 2013

Table 3. Sensitivity test scenarios for selected parameters.

Parameter	Base value	Changing(A)	Changing(B)	Changing(C)
r (CH_4/CO_2)	0.2	±0.5	±1.0	±1.5
Q10 (methane production)	2	±0.5	±1.0	±1.5
Q10 (methane oxidation)	2	±0.5	±1.0	–

GMDD
6, 5423–5473, 2013

Table 4. Calibrated values for the release ratio of CH_4 to CO_2 and Q10 parameters at each site.

ID	Sites	Location	r (CH_4/CO_2)	Q10
1	Sanjiang plain	China	0.45	3.5
2	Qinghai-Tibet	China	0.21	3
3	Stordalen	Sweden	0.5	2
4	Degero Stormyr	Sweden	0.2	2
5	Salmisuo mire	Finland	0.27	1.7
6	Ruovesi	Finland	0.14	1.6
7	Plotnikovo West Siberia	Russia	0.2	2
8	Florida	USA	0.15	3
9	Fairbanks Alaska	USA	0.2	2
10	Minnesota	USA	0.14	2.3
11	Michigan	USA	0.2	2
12	Sallies Fen	USA	0.2	2
13	Loch Vale,Colorado	USA	0.55	2
14	BOREAS SSA	Canada	0.2	2
15	BOREAS NSA	Canada	0.25	2
16	Quebec	Canada	0.2	3
17	Mer Bleue	Canada	0.1	3
18	Ryans 1 Billagong	Australia	0.35	3.5
19	Amazon basin	Brazil	0.15	4.5

GMDD
6, 5423–5473, 2013

Table 5. Modeled CH_4 emissions compared to observations in the Florida everglades.

References	Period	CH_4 Emissions $mg\,C\,m^{-2}\,day^{-1}$
Bartlett et al. (1989)	Jan–Feb 1984, Dec 1985	3.15~61.425
This study	Months above	0~77.7 Mean ± STD: 56.4 ± 18.9
Burke et al. (1988)	Jun, Nov 1986; Mar, Aug 1987	Mean: 21.75~481.5
This study	Months above	0~106.5 Mean ± STD: 62 ± 22.2
Harriss et al. (1988)	Jun 1980; May, Oct, Nov 1982; Jan, Feb 1984; Jan, Feb, Dec 1985	3~55.5
This study	Months above	0~97.0 Mean ± STD: 60.4 ± 20.9

GMDD
6, 5423–5473, 2013

Table 6. Modeled CH_4 emissions compared to observations in the Amazon Basin.

References	Period	CH_4 Emissions ($g C m^{-2} month^{-1}$)	Total CH_4 Emissions ($Tg C yr^{-1}$)
Devole et al. (1988)	Jul~Aug 1985	Flooded forests: 2.56 Macrophytes: 13.72	
Bartlett et al. (1988)	18 Jul~2 Sep 1985	Flooded forest: 4.46 Grass mats: 5.35	
This study	Jul~Aug 1985	4.68 ± 1.05	
Bartlett et al. (1990)	Apr~May 1987	Flooded forest: 2.93 Grass mats: 4.67	
This study	Apr~May 1987	2.98 ± 0.6	
Melack et al. (2004)			6.8
This study			6.32

GMDD
6, 5423–5473, 2013

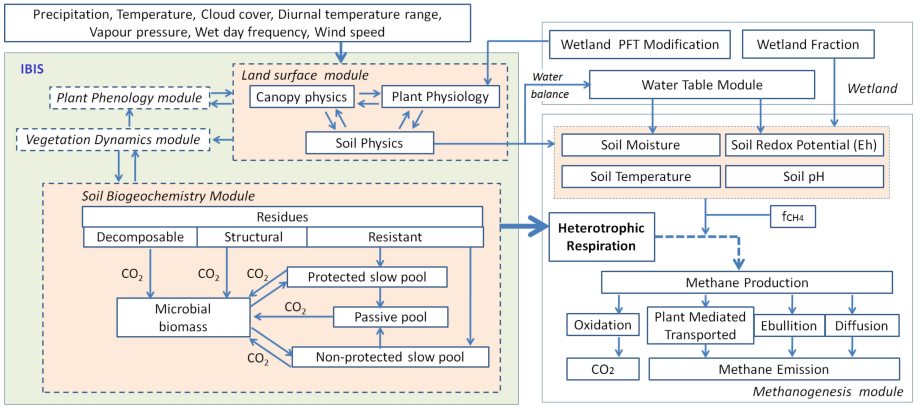

Fig. 1. Basic structural concept and integration of CH_4 emission and the water table modules into DGVM of IBIS in TRIPLEX-GHG.

GMDD
6, 5423–5473, 2013

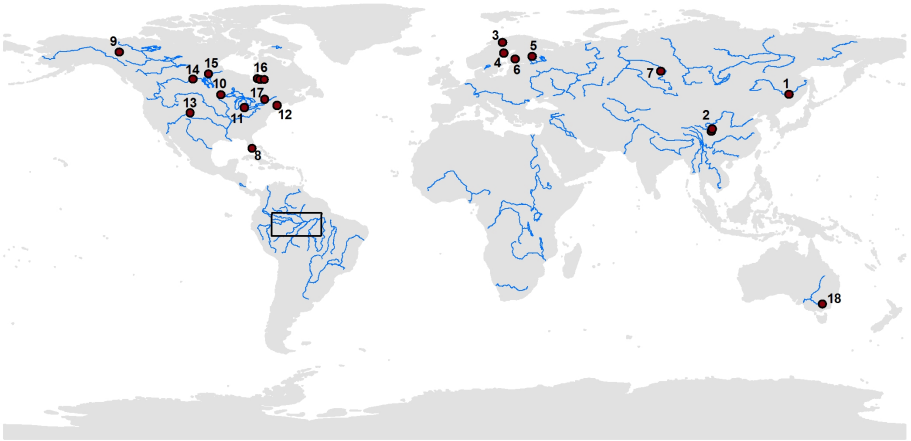

Fig. 2. Map of the sites for model parameter fitting and calibration. The ID numbers listed as in Table 1 were correspondingly marked.

GMDD
6, 5423–5473, 2013

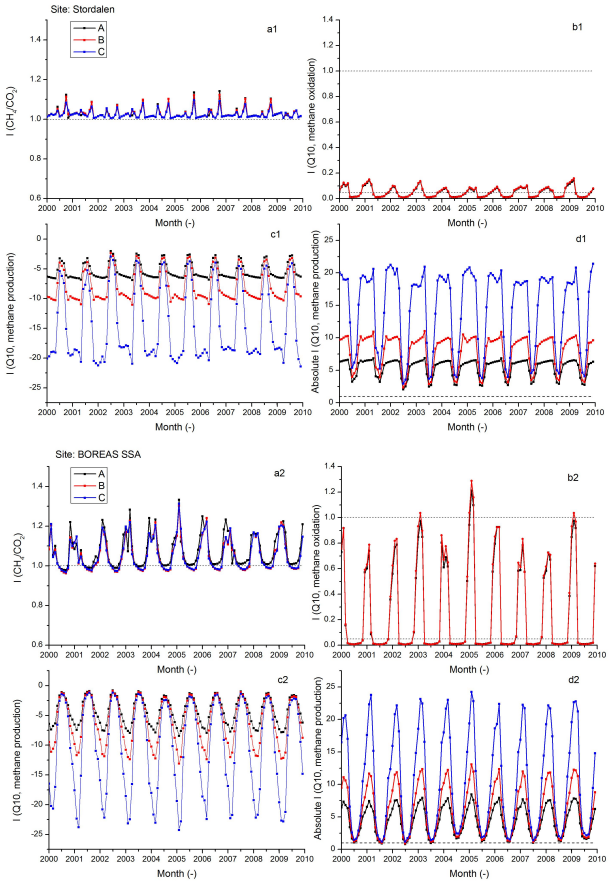

Fig. 3. Sensitivity analysis of the three parameters in the CH_4 module at two selected sites (Stordalen, BOREAS SSA). The ratio of CH_4 to CO_2 (**a1**, **a2**); Q10 for CH_4 oxidation (**b1**, **b2**); and the Q10 for CH_4 production (**c1**, **d1**; **c2**, **d2**). A, B, and C denote changing scenarios of the three parameters (see Table 3).

GMDD
6, 5423–5473, 2013

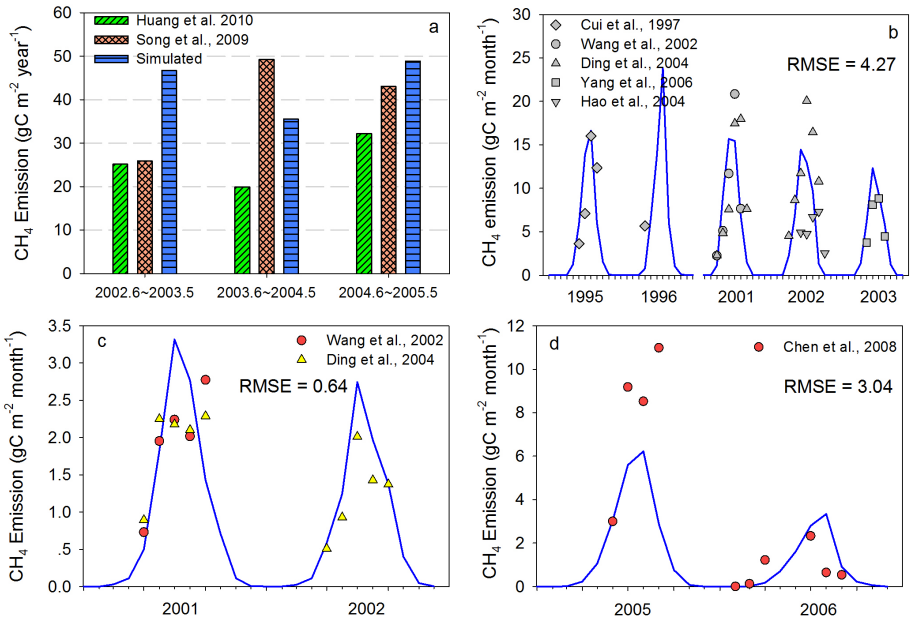

Fig. 4. Comparison of modeled and observed CH_4 emissions for the two selected sites in China.

GMDD
6, 5423–5473, 2013

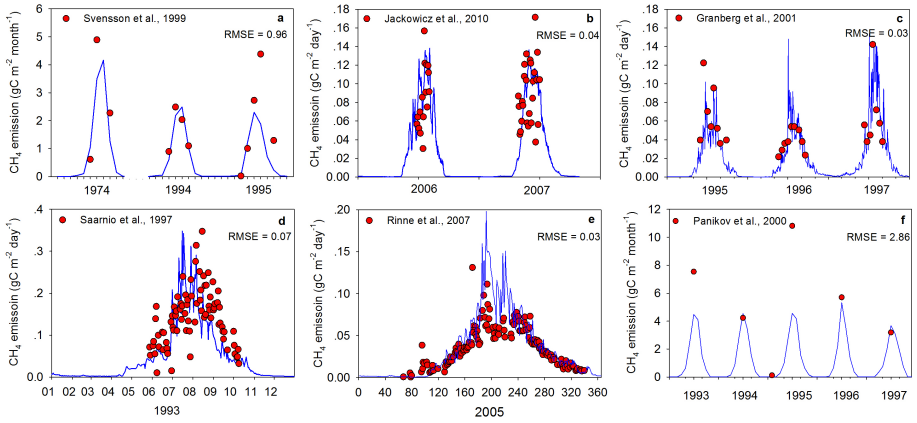

Fig. 5. Comparison of modeled and observed CH_4 emissions for the sites in Europe.

GMDD
6, 5423–5473, 2013

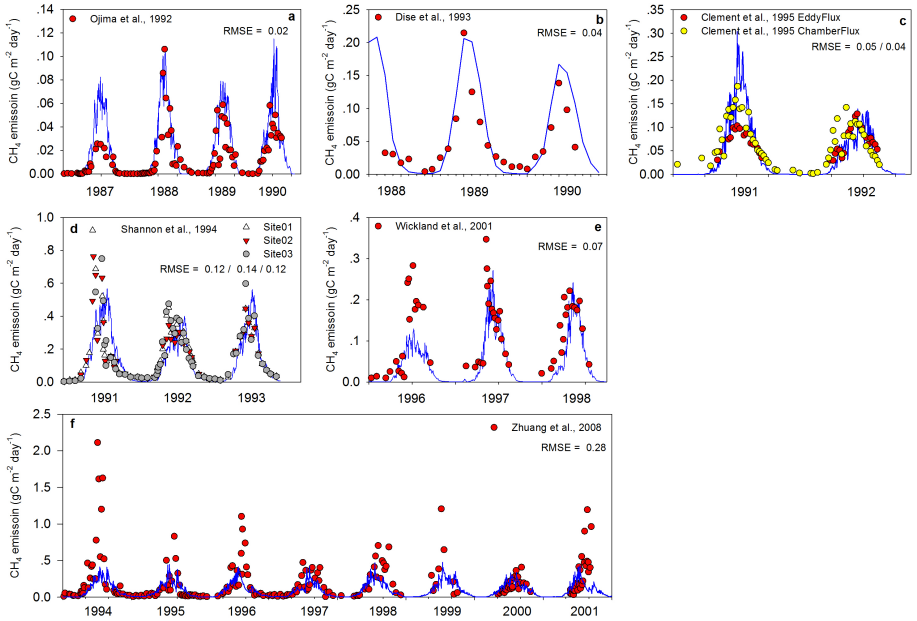

Fig. 6. Comparison of modeled and observed CH_4 emissions for the sites in the USA.

GMDD
6, 5423–5473, 2013

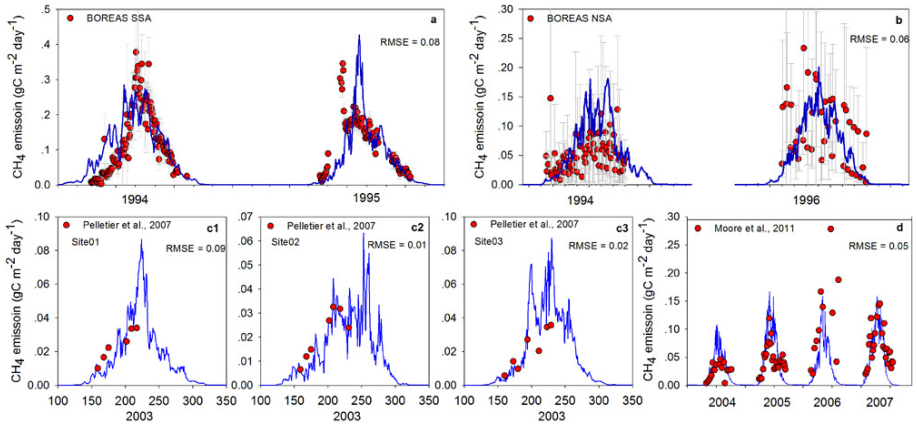

Fig. 7. Comparison of modeled and observed CH_4 emissions for the sites in Canada. Gray bars denote standard deviation in **(a)** and **(b)**.

GMDD
6, 5423–5473, 2013

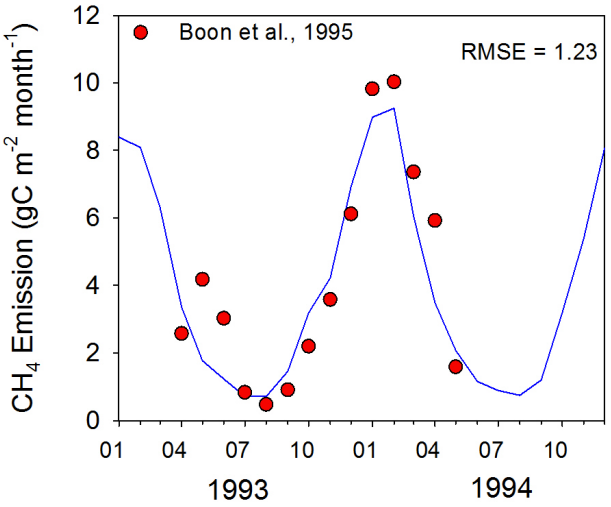

Fig. 8. Comparison of modeled and observed CH_4 emissions for the sites in Australia.

GMDD
6, 5423–5473, 2013